

Phase Behavior and Rheology of Blends Containing Polycarbonate and a Thermotropic Polyester

SUKMIN LEE,¹ PATRICK T. MATHER,^{1,2,*} and DALE S. PEARSON^{1,†}

¹Materials Research Laboratory and Materials Department, University of California, Santa Barbara, California 93106;

²USAF Phillips Laboratory, Fundamental Technologies Division, Edwards AFB, California 93524-7680

SYNOPSIS

The phase behavior and rheology of binary blends of polycarbonate (PC) and a liquid crystalline polymer (LCP) have been investigated. The thermotropic LCP employed was a semiflexible polyester synthesized by melt condensation of *t*-butylhydroquinone and 4,4'-dichloroformyl- α,ω -diphenoxyhexane. It shows a distinct nematic-to-isotropic transition in the pure state and in the blends. Results of DSC and optical microscopy indicate that the LCP is solubilized in the mixture for weight fractions of LCP less than about 0.05 and shows partial miscibility with PC over the rest of the composition range. The phase separation is considered to be driven by both isotropic and anisotropic interactions between constituent chains. Dynamic oscillatory measurements show that there is some interaction between the separate isotropic and anisotropic phases, with complex viscosities of the blends being intermediate between those of pure components and showing significant deviation from a logarithmic rule-of-mixtures. © 1996 John Wiley & Sons, Inc.

INTRODUCTION

Blends of liquid crystalline polymers (LCPs) with thermoplastic polymers offer novel properties, such as improved processibility and enhanced mechanical properties in the solid state after processing. For this reason, they have been the subject of active research interests in the past decade.^{1,2}

Blends studied often include typical thermotropic LCPs such as copolymers of hydroxybenzoic acid and hydroxynaphthoic acid (Vectra A series, Hoechst Celanese)³⁻¹¹ or copolymers of poly(ethylene terephthalate) (PET) and hydroxybenzoic acid (HBA).^{12,13} The Vectra A polymers usually feature a high melting point (T_m) ($\sim 280^\circ\text{C}$) and an inaccessible nematic-to-isotropic transition temperature (T_{ni}) due to degradation at temperatures below the isotropization temperature ($\sim 350^\circ\text{C}$). The PET/HBA copolymers show com-

plicated phase transitions and segregation, both effects being dependent on the copolymer composition. These observations have been recently confirmed and summarized by Brostow et al.¹⁴ Due to the complicated thermal behavior of the PET/HBA copolymers, rheological properties depend greatly on the thermal and mechanical histories which influence the crystalline and/or nematic structure.¹⁵⁻¹⁷

There has been some research^{18,19} dealing with blends containing LCPs with an accessible T_{ni} . The synthetic route used to lower T_{ni} has been the incorporation of flexible spacers in the main chain and/or random copolymerization in which the persistence length is lowered through backbone kinks. The particular LCPs used in these studies^{18,19} were still crystallizable and clearing (nematic-to-isotropic) transitions were not clearly detected with the DSC; however, polarizing optical microscopy of LCPs showed the biphasic texture present during the transition to the isotropic phase. The broad and obscure nematic-to-isotropic transition of these LCPs is probably due to "polyflexibility" or to the presence of nonuniformity of persistence length along the polymer backbones. This polyflexibility stems from the random nature of LCP chains re-

* To whom correspondence should be address at OLAC PL/RKFE, 10 E. Saturn Blvd., Edwards AFB, CA 93524-7680.

†Deceased.

sulting from copolymerization. Generally, semicrystalline LCPs show a narrow nematic phase region between a strong (large ΔH) melting and a relatively weak (small ΔH) nematic-to-isotropic transition.²⁰ In these cases, it is possible for crystallites of a higher melting temperature to grow within the nematic phase unless the samples are carefully annealed between the melting and clearing temperatures. This complication may affect blend behavior, including phase transitions and rheology. Broadening the nematic temperature range²¹⁻²⁵ of semicrystalline LCPs provides one method to minimize these problems.

The present study focuses on blends in which the liquid crystalline component shows a distinct nematic-to-isotropic transition, eliminating the complications discussed above. We chose a thermotropic liquid crystalline homopolyester which shows a narrow and strong nematic-to-isotropic transition with a relatively low transition temperature ($T_{ni} = 233^\circ\text{C}$).²⁶ We explored the phase behavior and linear viscoelastic properties of blends containing this LCP and polycarbonate.

EXPERIMENTAL

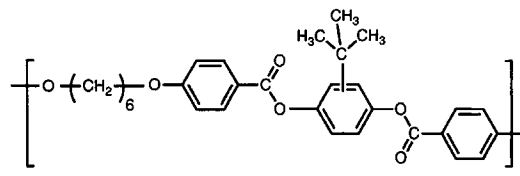
Materials

Polycarbonate (PC) was purchased from the Aldrich Chemical Co. The number- and weight-average molecular weight as provided by the supplier are 18,700 and 31,000, respectively. The liquid crystalline polyester was synthesized by melt condensation. The chemical formula of LCP employed is shown below.

The monomer synthesis and condensation reaction of this LCP have been described elsewhere.²⁶ Molecular weights based on polystyrene calibration are $M_n = 15,800$ and $M_w = 42,300$. A "monoflexible" LCP chain is achieved by maintaining the regular sequence of units along the chain. Bulky pendant groups on the main chain of the LCP prevent crystallization and enable the LCP to form only a glassy state with a glass transition temperature (T_g) of 90°C and a broad nematic phase (about 140°C between T_g and T_{ni}) in the pure state. The molecular, thermal, and rheological characterization of the LCP in the pure state are reported elsewhere.^{26,27}

Blending

Blends of various compositions were prepared by dissolving the desired amounts (w/w) of PC and



Chemical structure of LCP.

LCP in chloroform. The solutions were homogeneous and transparent. The solutions were cast on glass plates and the solvent evaporated, following which the films were dried in a vacuum oven at room temperature for 72 h.

Differential Scanning Calorimetry

Differential scanning calorimetry (DSC) was carried out using a Perkin-Elmer DSC-7. Indium [$T_m = 156.4^\circ\text{C}$, ΔH_f (heat of fusion) = 28.45 J/g] was used as a standard for calibration. All experiments were carried out under a constant flow of dry nitrogen. Sample weights ranged from 18 to 20 mg, and the heating rate was $10^\circ\text{C}/\text{min}$. The T_g was defined as the temperature corresponding to the half-height of the heat capacity change, and the T_{ni} , as the maximum of the transition peak on heating. Data reported here were taken from second heating runs made after maintaining samples at 265°C for 4 min and cooling with an ice/water mixture used as the DSC reservoir.

Optical Microscopy

The blends were observed using a Nikon Optiphot-Pol optical microscope with a tungsten lamp illumination equipped with a Mettler hot stage (FP-82) with or without crossed polarizer and analyzer. The films were prepared by evaporating solutions of mixtures in chloroform onto microscopy slides, yielding thicknesses of 50–70 microns. The films were observed at a magnification of $200\times$ and photographs were taken with a Nikon 8008 camera.

Rheological Measurement

Dynamic oscillatory shear measurements were performed using a Rheometrics RMS-800 mechanical spectrometer equipped with 25 mm-diameter parallel plates. Discs about 1.2 mm thick and 25 mm in diameter were molded at $220\text{--}240^\circ\text{C}$, depending on the blend composition, using flakes from films that had been cast from solution and vacuum-dried

for 72 h at room temperature. After clearing the thermal history of the LCP-rich phase by annealing samples for 20 min at 270°C ($>T_{ni}$), linear viscoelastic measurements were performed from 265 to 180°C with temperature spacing of 5°C. Strain amplitude sweeps were conducted to determine the best oscillation amplitude such that results were independent of amplitude and that sufficient torque was generated at the lowest frequencies. The angular velocity was varied from 0.1 to 100 rad/s, and the cooling rate was about 1°C/min. Thermal equilibrium was assured by using a dwell time before each measurement of at least 5 min. The gap between shearing surfaces was adjusted to compensate for thermal contraction of the sample and shearing fixtures upon cooling.

RESULTS AND DISCUSSION

The thermal behavior and morphology of blends were investigated with DSC and optical microscopy. Figure 1 contains typical DSC thermograms showing the glass transition and the nematic-to-isotropic transition of LCP/PC mixtures with various compositions. The T_g of the pure LCP is about 90°C. The peak at 233°C of the pure LCP is attributed to the nematic–isotropic transition and was confirmed by the elimination of birefringence on heating. The broadness of the peak is most likely due to the sample polydispersity ($M_w/M_n = 2.67$) typical of polycondensation polymers, the shorter chains clearing at a lower temperature than that of the longer chains. The nematic temperature range is large due to the suppression of crystallization, with the temperature difference from T_g to T_{ni} being about 140°C. The pure PC shows a T_g of 146°C as reported in the literature.²⁸ In LCP/PC blends with the weight fraction of LCP (w_{LCP}) greater than or equal to 0.1, two T_g 's and a T_{ni} peak appear in the DSC traces. For w_{LCP} equal to 0.05, the peak of T_{ni} disappears completely and a single T_g is observed, corresponding to that of a PC-rich phase.

Observations with polarizing microscopy of a sample with $w_{LCP} = 0.05$ showed no trace of birefringence from room temperature to 265°C. This, along with the observation of a single T_g , indicates that the LCP is dissolved completely in the isotropic PC matrix. Blends with $w_{LCP} > 0.05$ show phase separation as evidenced by the coexistence of both highly birefringent (nematic) and dark (isotropic) regions from room temperature to temperatures near T_{ni} . The highly birefringent domains shrink on ap-

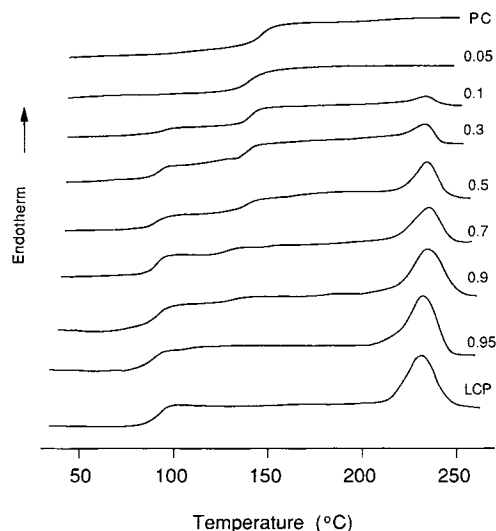


Figure 1 Typical DSC thermograms showing transition temperatures of LCP/PC blends at various blend compositions. Numbers on the figure denote the weight fraction of LCP.

proaching T_{ni} and completely disappear above T_{ni} . Above T_{ni} , for all blend compositions, no interfaces were observed with or without the analyzer in place above the sample.

Figure 2 (a)–(c) display photomicrographs for several blend compositions showing separation of the birefringent nematic (LCP-rich) and the isotropic (PC-rich) phases at 180°C. The length scale characterizing the heterogeneity is about 10–30 microns. The isotropic domains form rather discretely in the nematic matrix for $w_{LCP} = 0.7$ [Fig. 2(a)], while the nematic phase is co-continuous for $w_{LCP} = 0.5$ and $w_{LCP} = 0.3$ [Fig. 2(b) and (c), respectively]. It should be noted that our samples displayed considerable heterogeneity in morphology and photomicrographs were taken of the most representative areas. The observed morphological difference between the $w_{LCP} = 0.7$ and $w_{LCP} = 0.3$ blends is due, in part, to the viscosity mismatch ($p = \eta_{minor}/\eta_{major}$) of the component polymers in the blends.²⁹ The viscosity of the PC sample is roughly two orders of magnitude higher than that of the LCP used in this study. With such a significant viscosity mismatch, the morphology of the blends does not lose memory of the solvent-casting process over the time scale of the experiment. Another factor influencing the morphology of the phase-separated blends is the anisotropic nature of interfacial tension between the nematic and isotropic phases, which may influence whether the minor phase would minimize free energy by forming a co-continuous morphology vs. a dis-

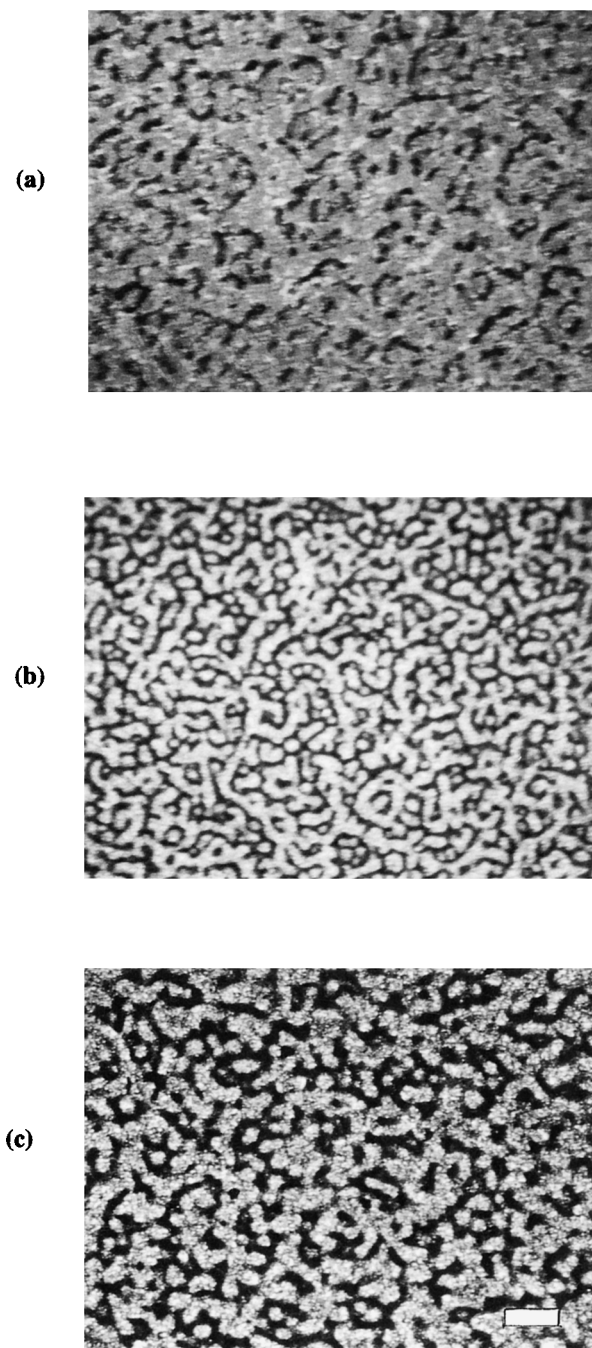


Figure 2 Polarizing optical microscopic photographs showing biphases of LCP/PC blends with (a) $w_{\text{LCP}} = 0.7$, (b) $w_{\text{LCP}} = 0.5$, and (c) $w_{\text{LCP}} = 0.3$, taken after annealing at 180°C for 200 min. White bar on the figure indicates 50 microns.

crete morphology. This is the area that we are currently studying.

It is concluded from the preceding that the LCP is miscible in PC for small weight fractions (w_{LCP}

< 0.05), but features both nematic and isotropic phases for larger weight fractions of LCP. Similar behavior has been observed in other LCP/thermoplastic polymer mixtures.¹⁹

The T_g trend of LCP/PC blends obtained from DSC traces is summarized in Figure 3. The T_g of the LCP-rich phase is nearly independent of blend composition and has a value near 90°C. The invariance of the lower T_g indicates that this phase is composed of almost pure LCP. The T_g of the PC-rich phase decreases slightly with increasing w_{LCP} . This indicates partial miscibility of the LCP in PC which may originate from the formation of an electron-transfer complex commonly present in blends containing aromatic polymers with ester or carbonate linkages.¹⁸ We are currently unable to explain the downward trend in the PC-rich T_g for large values of w_{LCP} . The implication is that the solubility of LCP chains in PC increases for $w_{\text{LCP}} > 0.7$.

In Figure 4, we present the T_{ni} and enthalpies of isotropization (ΔH_{ni}) of LCP/PC blends as determined by DSC. T_{ni} is almost independent of blend composition, maintaining the value of 233°C corresponding to pure LCP. However, the quantity $\Delta H_{\text{ni,blend}}/w_{\text{LCP}}$ —or Joules per gram of LCP added to the blend—decreases continuously to zero upon varying the LCP weight fraction, w_{LCP} , from 1 to 0.05. If all the LCP molecules added to the blend were in the nematic phase, this quantity would not depend on w_{LCP} , as shown with the dotted line in Figure 4. The observed trend, therefore, can be explained by an increasing fraction of LCP dissolved in the PC-rich phase with decreasing LCP composition. The invariance of T_{ni} shows that the LCP-rich nematic phase is nearly free of PC molecules for all weight fractions. These show qualitatively that the blends were separated into phases of an almost pure LCP phase and a PC-rich phase which contained a significant number of LCP molecules (see phase diagram of Fig. 5 discussed below).

Figure 5 is the phase diagram of our LCP/PC binary blends based on the results of DSC analysis and optical microscopy. The points on the diagram are the locations of peaks on DSC traces and the identification of each phase was performed using polarizing optical microscopy. The miscibility of the isotropic–isotropic mixture of melts above T_{ni} was confirmed by the visual observation (direct and magnified) that thin films of the blends were completely transparent above 250°C.

Dynamic oscillatory measurements were used to characterize rheological properties of the nematic, isotropic, and biphasic regions in the LCP/PC

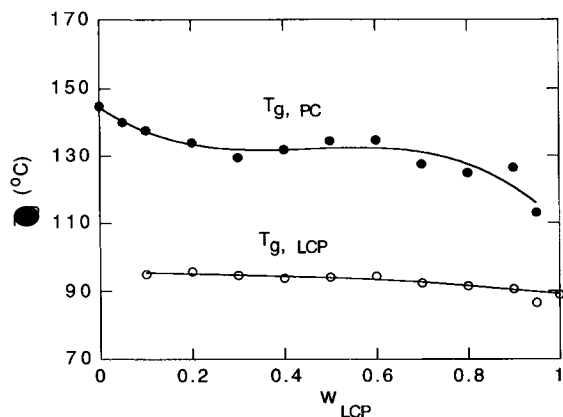


Figure 3 The T_g of LCP/PC blends measured during second heating with DSC at the heating rate $10^\circ\text{C}/\text{min}$ after cooling from 265°C at which samples were annealed for 4 min.

blends. Figure 6(a) and (b) shows the storage and loss moduli vs. frequency for various blend compositions at 180°C and 200°C , respectively. Time-temperature superposition (TTS) is not generally applicable to LCP blends, due to the anisotropic character of the LCP and the phase segregation. We did not vary temperature over a wide enough range to check this, however, for two reasons: First, the lowest temperature for linear viscoelastic measurements was limited to 180°C , below which the torque was too high to detect since the T_g of PC is about 150°C . Second, the LCP-rich phase begins the nematic-isotropic phase transition near 210°C , as shown in Figure 1. Although the moduli could be superposed within the temperature range of 180 – 200°C using frequency shifting [see Fig. 6(a) and (b)], it was

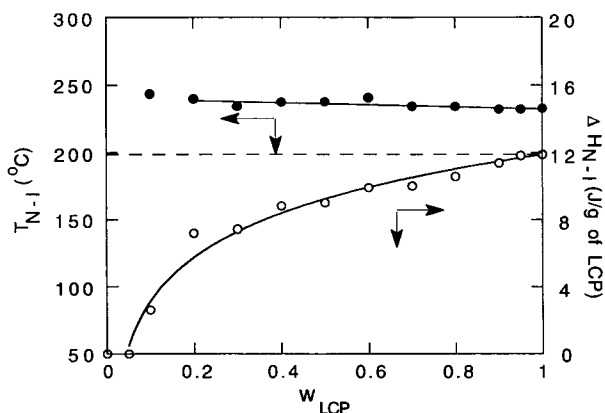


Figure 4 The T_{ni} and ΔH_{ni} of LCP/PC blends measured during second heating with DSC. The dotted line denotes the ideal enthalpy of nematic-to-isotropic transition (see text).

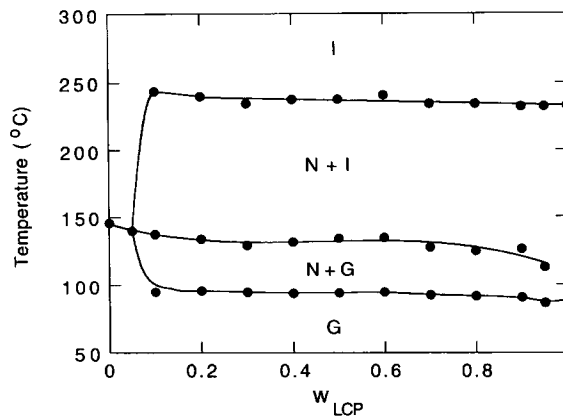


Figure 5 Apparent phase diagram of LCP/PC blends constructed from DSC and optical microscopy. Isotropic, nematic, and glassy phases are denoted by I, N, and G, respectively.

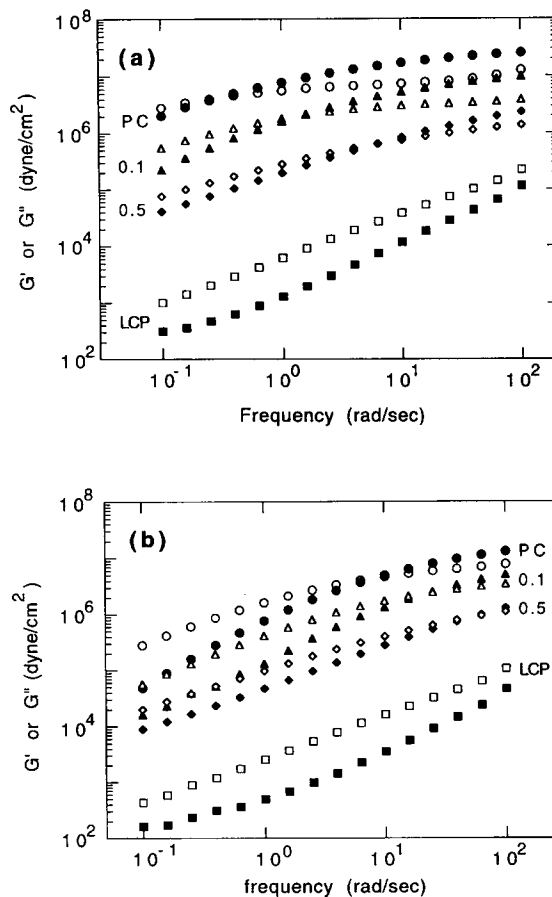


Figure 6 Storage and loss moduli at the various composition of LCP/PC blends measured in biphasic region of (a) 180°C and (b) 200°C . Numbers on the figures denote the LCP weight fraction. Black and white symbols denote the G' and G'' , respectively, at each composition.

too small of a temperature range to extract a definite conclusion regarding applicability of TTS to these blends. The data do suggest, however, that the two phases relax over similar time scales and that the character of the liquid crystalline phase is not altered much over the temperature range studied.

The loss moduli, $G''(\omega)$, in the pure LCP are about two to five times higher than the storage moduli, $G'(\omega)$, over the entire frequency range. Also, G'' was found to scale with frequency as, $G'' \sim \omega^{0.8}$, while the storage modulus, G' , changed slope over the entire frequency range. This behavior is similar to that observed for other thermotropic melts.^{17,30,31}

As shown in Figure 6(a), the mechanical spectrum of the pure PC displays a rubbery plateau typical of flexible polymer melts. The blend with $w_{\text{LCP}} = 0.1$ exhibits values of G' and G'' lower than in the pure PC and higher than in the pure LCP. It also shows the approach toward terminal or viscous behavior at low frequencies. The cross-point of G' and G'' curves shift to a higher frequency in comparison to the pure PC, indicating a decrease in the longest relaxation time of the blend. This trend—decreasing moduli and increasing relaxation time—is continued as the weight fraction of LCP is increased to 0.5. Overall moduli decrease monotonically with increasing w_{LCP} , but do not follow a simple mixing rule. The failure to obey a simple mixing rule may be attributed to the influence of interfacial tension on the rheological properties.

Figure 6(b) shows the longer relaxation time behavior of pure PC close to the terminal zone at the higher temperature (200°C). As the LCP composition increases, the slope of G'' becomes smaller than in the pure PC but still larger than in the pure LCP. This is considered to be the intermediate behavior stemming from the partial miscibility of the two components. It may also be argued that there is an increase in the molecular weight between entanglements, M_e , of PC chains in the presence of the semiflexible LCP chains; however, we have no direct evidence to support this argument.

Plotted in Figure 7 is the complex viscosity, $|\eta^*(\omega (\omega = 1 \text{ rad/s}))|$, as a function of temperature during cooling between 265 and 180°C with a cooling rate of 1°C/min. For pure PC, the viscosity increases with decreasing temperature, in a manner similar to most liquids. For pure LCP, however, the viscosity begins to fall with decreasing temperature near 240°C—the same temperature as the isotropic-to-nematic phase transition. The viscosity continues to decline until about 220°C, at which point the phase transition is complete,

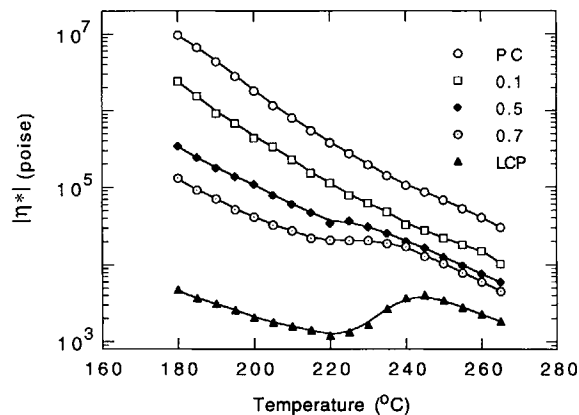


Figure 7 Dynamic viscosity at the various blend composition measured at 1 rad/s during cooling after annealing 20 min at 270°C. Numbers on the figures denote the LCP weight fraction.

and the viscosity begins to rise with decreasing temperature. The finite temperature range over which viscosity decreases during cooling is due primarily to polydispersity of the LCP. The viscosity drop on cooling past the isotropic-nematic phase transition is a flow characteristic common to thermotropic liquid crystalline materials featuring an accessible clearing transition.³²

In the case of w_{LCP} of 0.7, a similar but less dramatic viscosity change is observed. This behavior is consistent with our polarizing microscopy observations which showed that isotropic/nematic phase separation occurs during cooling in the blends below the isotropic-nematic transition temperature of the pure LCP. The reduction in viscosity with decreasing temperature of the LCP-rich phase is compensated by the increasing viscosity of the PC-rich phase, so that the viscosity appears to remain unchanged for a certain range of temperatures. This behavior is diminished as the PC content increases, since the viscosity of the PC-rich phase dominates at low LCP composition. The temperature dependence of viscosity for the $w_{\text{LCP}} = 0.1$ blend is similar to that of pure PC, but shows considerably reduced values.

The complex viscosity as a function of the blend composition at 180°C is shown in Figure 8, with the oscillation frequency as a parameter. The blend viscosity, $|\eta^*|$, decreases continuously with the addition of the LCP, showing values intermediate between those of the pure components. For small LCP compositions, the viscosity decreases rather steeply with increasing w_{LCP} . It appears that the LCP molecules dissolved in the PC-rich phase within the

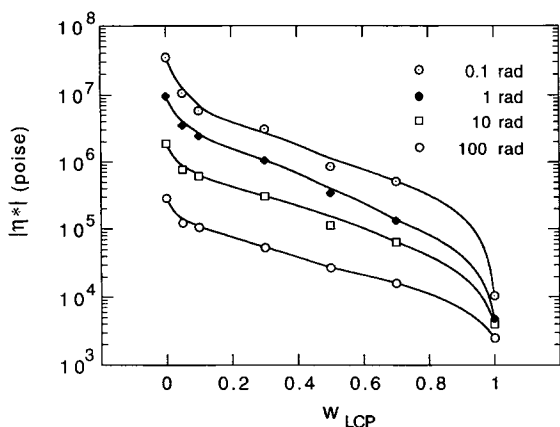


Figure 8 Dynamic viscosity of LCP/PC blends with respect to the blend composition at several frequencies.

miscible composition range act to plasticize the blends. Larger LCP compositions for which phase separation occurs show a smaller negative slope on the viscosity–composition curve. Finally, a large drop in viscosity at large LCP compositions is observed for all oscillation frequencies.

On the whole, our measurements of the complex viscosity in these blends follow neither a logarithmic rule-of-mixtures relation ($\log \eta = w_1 \cdot \log \eta_1 + w_2 \cdot \log \eta_2$) nor an inverse rule-of-mixtures expression ($1/\eta = w_1/\eta_1 + w_2/\eta_2$). The viscosity trends were observed to deviate more from the logarithmic rule-of-mixtures at lower frequencies. This is likely due to the fact that oscillatory shear at lower frequencies probes time scales comparable to the relaxation time of the phase-separated morphology, while high frequencies probe the shorter relaxation times of molecular length scales.³³

CONCLUSION

The phase behavior and rheology of binary blends of polycarbonate (PC) and a liquid crystalline polymer (LCP) were investigated. The thermotropic LCP employed showed a distinct nematic-to-isotropic transition in the pure state and in the blends. Results of DSC and optical microscopy have indicated that the LCP is solubilized in the mixture for weight fractions of LCP less than about 0.05 and shows partial miscibility with PC over the rest of the composition range. Dynamic oscillatory measurements have shown that there is some interaction between the separate isotropic and anisotropic phases, with complex viscosities of the blends being

intermediate between those of pure components. Future work is under way to measure the interfacial tension between the blend components of this study and to develop an emulsion model describing the linear viscoelastic behavior of LCP-flexible polymer blends.

The authors gratefully thank B. Riise for stimulating discussion. This work was supported by the MRL Program of the National Science Foundation under Grant Award No. DMR-9123048.

REFERENCES

1. D. Dutta, H. Fruitwala, A. Kohli, and R. Weiss, *Polym. Eng. Sci.*, **30**, 1005 (1990).
2. W. Brostow, *Polymer*, **31**, 779 (1990).
3. L. Incarnato, M. R. Nobile, and D. Acierno, *Makromol Chem. Macromol Symp*, **68**, 277 (1993).
4. W. N. Kim and M. M. Denn, *J. Rheol.*, **36**, 1477 (1992).
5. H. Verhoogt, H. C. Langelaan, J. Van Dam, and A. Posthuma de Boer, *Polym. Eng. Sci.*, **33**, 754 (1993).
6. F. P. La Mantia, F. Cangialosi, U. Pedreltti, and A. Roggero, *Eur. Polym. J.*, **29**, 671 (1993).
7. A. Siegmund, A. Dagan, and S. Kenig, *Polymer*, **26**, 1325 (1985).
8. A. Mehta and A. I. Isayev, *Polym. Eng. Sci.*, **31**, 971 (1991).
9. F. P. La Mantia and A. Valenza, *Makromol Chem. Macromol Symp*, **56**, 151 (1992).
10. J. Seppala, M. Heino, and C. Kapanen, *J. Appl. Polym. Sci.*, **44**, 1051 (1992).
11. W. G. Perkins, A. M. Marcelli, and H. W. Frerking Jr., *J. Appl. Polym. Sci.*, **43**, 329 (1991).
12. A. Aji and P. A. Gignac, *Polym. Eng. Sci.*, **32**, 903 (1992).
13. E. Amendola, C. Carfagna, P. Netti, L. Nicolais, and S. Saiello, *J. Appl. Polym. Sci.*, **50**, 83 (1993).
14. W. Brostow, M. Hess, and B. L. Lopez, *Macromolecules*, **27**, 2262 (1994).
15. Y. G. Lin and H. H. Winter, *Macromolecules*, **24**, 2877 (1991).
16. T. Sun, Y. G. Lin, H. H. Winter, and R. S. Porter, *Polymer*, **30**, 1257 (1989).
17. D. S. Kalika, D. W. Giles, and M. M. Denn, *J. Rheol.*, **34**, 139 (1990).
18. Y. G. Lee, H. W. Lee, H. H. Winter, S. Dashevsky, and K. S. Kim, *Polymer*, **34**, 4703 (1993).
19. H. G. Schild, E. S. Kolb, R. A. Gaudiana, Y. Chiang, and W. C. Schwarzl, *J. Appl. Polym. Sci.*, **46**, 959 (1992).

20. S. Drappel, B. W. A. Yeung, P. R. Sundararajan, A. Rudin, *J. Rheol.*, **37**, 89 (1993).
21. S. S. Kim and C. D. Han, *Macromolecules*, **26**, 3176 (1993).
22. S. S. Kim and C. D. Han, *Macromolecules*, **26**, 6633 (1993).
23. C. D. Han and S. S. Kim, *J. Rheol.*, **37**, 847 (1993).
24. C. D. Han and S. S. Kim, *J. Rheol.*, **38**, 13 (1994).
25. C. D. Han and S. S. Kim, *J. Rheol.*, **38**, 31 (1994).
26. P. T. Mather et al., *Liq. Cryst.*, **17**, 811 (1994).
27. P. T. Mather, S. Lee, and N. Grizutti, to appear.
28. J. Brandrup and E. H. Immergut, *Polymer Handbook*, 3rd ed., Wiley-Interscience, New York, 1989.
29. L. A. Utracki, *J. Rheol.*, **35**, 1615 (1991).
30. D. S. Kalika, L. Nuel, and M. M. Denn, *J. Rheol.*, **33**, 1059 (1989).
31. K. F. Wissburn, *Br. Polym. J.*, **12**, 163 (1980).
32. R. S. Porter and J. F. Johnson, *Rheology, Vol 4*, F. R. Eirich, Ed., Academic Press, New York, 1967.
33. J. D. Ferry, *Viscoelastic Properties of Polymers*, 3rd ed., Wiley-Interscience, New York, 1980.

Received April 27, 1995

Accepted June 28, 1995